NONLINEAR VIBRATIONS OF AN AXIALLY EXCITED CIRCULAR CYLINDRICAL SHELL CONSIDERING THE EFFECTS OF MODAL COUPLING

Frederico M. A. Silva*[1]**, Lara Rodrigues**[1]**, Paulo B. Gonçalves**[2]**, Zenón J. G. N. Prado**[1]

[1]School of Civil Engineering, Federal University of Goiás, Brazil.
silvafma@eec.ufg.br, lara.rdgs@gmail.com, zenon@eec.ufg.br

[2] Department of Civil Engineering, Pontifical Catholic University of Rio de Janeiro, Brazil.
paulo@puc-rio.br

Keywords: Modal Coupling, Nonlinear Analysis, Cylindrical Shells, Stability Boundaries, Basin of Attractions.

Abstract. *Cylindrical shells exhibit a dense frequency spectrum, especially near the lowest frequency range. In addition, due to the circumferential symmetry, frequencies occur in pairs. So, in the vicinity of the lowest natural frequencies, several equal or nearly equal frequencies may occur, leading to a complex dynamic behavior. So, the aim of the present work is to investigate the dynamic behavior and stability of cylindrical shells under axial forcing with multiple equal or nearly equal natural frequencies. The shell is modelled using the Donnell nonlinear shallow shell theory and the discretized equations of motion are obtained by applying the Galerkin method. For this, a modal solution that takes into account the modal interaction among the relevant modes and the influence of their companion modes (modes with rotational symmetry) which satisfies the boundary and continuity conditions of the shell is derived. Special attention is given to the 1:1:1:1 internal resonance (four interacting modes), a problem not treated in the technical literature. Solving numerically the governing equations of motion and using several tools of nonlinear dynamics, a detailed parametric analysis is conducted to clarify the influence of the internal resonances on the bifurcations, stability boundaries, nonlinear vibration modes and basin of attraction of the structure.*

1 INTRODUCTION

Thin-walled cylindrical shells are usually used to withstand axial loads and lateral pressure. Under these loading conditions they display an unstable post-buckling behavior. It is a well-known fact that this is due to the phenomenon of modal coupling, particularly the nonlinear coupling between the basic buckling mode and an axisymmetric mode with twice the number of waves in the axial direction as the buckling mode [1]. This modal coupling has also shown to be essential to correctly describe the nonlinear vibrations of cylindrical shells [2-4]. The consideration of axi-symmetric modes is necessary to describe the inherent in-out asymmetry observed in the nonlinear vibration and buckling pattern of the shell at large amplitudes. These shells may also exhibit several modes with the same or nearly the same critical loads, leading to a strong nonlinear interaction [5]. So, the development of consistent modal solutions capable of describing the main modal interactions observed in cylindrical shells has received much attention in literature. A detailed review of this subject, including more than 350 papers, was published in 2003 by Amabili and Païdoussis [6].

Cylindrical shells also exhibit a dense frequency spectrum, especially near the lowest frequency range. In addition, due to the circumferential symmetry, frequencies occur in pairs. So, in the vicinity of the lowest natural frequencies, several equal or nearly equal frequencies may occur. This closeness is even greater when one considers a static compressive loading. This may lead to a strong nonlinear interaction among these modes under dynamic conditions, influencing thereby the response and safety of the shell. Although there are many papers on modal coupling and interaction in the presence of static loads, little is known on their influence on the dynamic stability of thin-walled cylindrical shells. So, when considering the effect of nonlinearity, there is the possibility of interaction between the different non-linear vibration modes, which can cause significant changes in the stability boundaries and bifurcation diagrams [7-12]. However, no consistent modal solution taking into account the simultaneous effect of modal coupling plus modal interaction is found in literature [10, 11].

So the aim of the present work is (a) to deduce a consistent modal solution for a shell where two modes exhibits equal natural frequencies, retaining all modes that appear due to the nonlinear modal coupling and modal interaction, (b) obtain from this general expression a precise low order model for large amplitude vibrations, and (c) use this modal solution to study the nonlinear oscillations and instabilities of these cylindrical shells under axial loads. This modal solution is obtained by applying perturbation techniques, as suggested previously by the authors in [12, 13].

2 PROBLEM FORMULATION

2.1 Shell equations

Consider a perfect thin-walled circular cylindrical shell of radius R, length L, and thickness h. The shell is assumed to be made of an elastic, homogeneous, and isotropic material with Young's modulus E, Poisson ratio v and density ρ. The axial, circumferential and lateral coordinates are denoted by, respectively, x, θ and z, and the corresponding displacements on the shell surface are in turn denoted by u, v, and w, as shown in Figure 1.

The nonlinear equations of motion based on the Von Karmán-Donnell shallow shell theory, in terms of a stress function F and the transversal displacement w are given by:

$$\rho\,h\,\ddot{w} + \beta_1\,\rho\,h\,\omega_0\,\dot{w} + \beta_2\,D\,\nabla^4\dot{w} + D\nabla^4 w =$$

$$\frac{\left(F_{,\theta\theta} - P(t)\right)}{R^2}w_{,xx} - 2\frac{F_{,x\theta}}{R}\frac{w_{,x\theta}}{R} + F_{,xx}\left(\frac{w_{,\theta\theta}}{R^2} + \frac{1}{R}\right) \tag{1}$$

$$\frac{1}{Eh}\nabla^4 F = -\frac{1}{R}w_{,xx} - w_{,xx}\frac{w_{,\theta\theta}}{R^2} + \left(\frac{w_{,x\theta}}{R}\right)^2 \tag{2}$$

where β_1 and β_2 are, respectively, the linear viscous damping and the viscoelastic material damping coefficients, $D = E\,h^3/12(1-v^2)$ is the flexural stiffness of the shell, ω_0 is the lowest vibration frequency, $P(t)$ is the axial load and ∇^4 is the bi-harmonic operator defined as $\nabla^4 = \left[\partial^2/\partial x^2 + \partial^2/R^2\,\partial\theta^2\right]^2$.
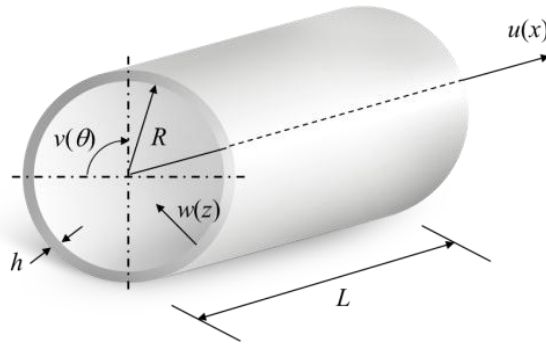

Figure 1: Geometry and displacement field of the cylindrical shell.

The shell is subjected to a harmonic axial load, uniformly applied at the edges, of the form:

$$P = P_0 + P_1\cos\left(\omega_f\,t\right) \tag{3}$$

For a simply-supported shell, the following boundary conditions must be satisfied in the transversal direction:

$$w(0,\theta) = w(L,\theta) = 0 \text{ and } M_x(0,\theta) = M_x(L,\theta) = 0 \tag{4}$$

In the foregoing, the following non-dimensional parameters have been introduced:

$$W = \frac{w}{h};\ \varepsilon = \frac{x}{L};\ \tau = \omega_0\,t;\ \Omega_f = \frac{\omega_f}{\omega_0};\ \Gamma_0 = \frac{P_0}{P_{CR}} \text{ and } \Gamma_1 = \frac{P_1}{P_{CR}} \tag{5}$$

Here $P_{CR} = E\,h^2/[R\,(3-3v^2)^{1/2}]$ is the classical axial buckling load of the shell [5].

2.2 General solution of the shell displacement field by a perturbation technique

As an example, consider a simply supported cylindrical shell with radius $R = 0.2$ m, $L = 0.34163$ m and $h = 0.002$ m. The shell material is homogeneous and isotropic with Young´s modulus $E = 210$ GPa, Poisson's ratio $v = 0.3$ and density $\rho = 7850$ kg/m³. The vibration modes of simply-supported cylindrical shells exhibit m half-waves in the axial direction and n waves in the circumferential direction. For this geometry the values of the lowest natural frequencies for modes $(m, n) = (1, 5)$ and $(m, N) = (1, 6)$ are 3799.03 rad/s [13]. So, this cylindrical shell has two distinct vibration modes with the same natural frequency. In addition, due to the circumferential symmetry, frequencies occur in pairs. This leads to a 1:1:1:1 internal resonance.

A detailed parametric analysis has shown that a large number of practical cylindrical shell geometries have four neighbor modes with the same natural frequencies. For the application of perturbation techniques, the analysis must begin by considering these four interacting modes as the modal initial solution (seed modes) in the perturbation procedure, i.e. [12, 13]:

$$
\begin{aligned}
W = & A1_{11}(\tau)\cos(n\theta)\sin(m\pi\varepsilon) + B1_{11}(\tau)\sin(n\theta)\sin(m\pi\varepsilon) \\
& + A2_{11}(\tau)\cos(N\theta)\sin(m\pi\varepsilon) + B2_{11}(\tau)\sin(N\theta)\sin(m\pi\varepsilon)
\end{aligned}
\tag{6}
$$

where $N = n+1$ and $A1_{11}(\tau)$, $A2_{11}(\tau)$, $B1_{11}(\tau)$ and $B2_{11}(\tau)$ are the time dependent modal amplitudes.

By applying the perturbation procedures, as described in [12, 13], and by considering the boundary conditions for a simply supported cylindrical shell, Eq. (4), the following modal solution that accounts for the modal coupling and interaction is obtained for the transversal displacement:

$$
\begin{aligned}
W = & \sum_{i=1,3,5}^{\overline{N}_1}\sum_{j=1,3,5}^{\infty}\Big[A1_{ij}(\tau)\cos(in\theta) + B1_{ij}(\tau)\sin(in\theta) \\
& + A2_{ij}(\tau)\cos(iN\theta) + B2_{ij}(\tau)\sin(iN\theta)\Big]\sin(jm\pi\varepsilon) \\
& + \sum_{i=1,2,3}^{\overline{N}_1-1}\sum_{j=1,3,5}^{\infty}\Big\{A3_{ij}(\tau)\cos\big[\big(iN-(\overline{N}_1-i)n\big)\theta\big] + B3_{ij}(\tau)\sin\big[\big(iN-(\overline{N}_1-i)n\big)\theta\big] \\
& + A4_{ij}(\tau)\cos\big[\big(iN+(\overline{N}_1-i)n\big)\theta\big] + B4_{ij}(\tau)\sin\big[\big(iN+(\overline{N}_1-i)n\big)\theta\big]\Big\}\sin(jm\pi\varepsilon) \\
& + \sum_{\alpha=0,2,4}^{\overline{N}_2}\sum_{\beta=0}^{\infty}\Big[A5_{\alpha(2+6\beta)}(\tau)\cos(\alpha n\theta) + B5_{\alpha(2+6\beta)}(\tau)\sin(\alpha n\theta) \\
& + A6_{\alpha(2+6\beta)}(\tau)\cos(\alpha N\theta) + B6_{\alpha(2+6\beta)}(\tau)\sin(\alpha N\theta)\Big]\times \\
& \left\{-\frac{(3+6\beta)}{(4+12\beta)}\cos(6\beta m\pi\varepsilon) + \cos[(2+6\beta)m\pi\varepsilon] - \frac{(1+6\beta)}{(4+12\beta)}\cos[(4+6\beta)m\pi\varepsilon]\right\} \\
& + \sum_{\alpha=1,2,3}^{\overline{N}_2-1}\sum_{\beta=0}^{\infty}\Big\{A7_{\alpha(2+6\beta)}(\tau)\cos\big[\big(\alpha N-(\overline{N}_2-\alpha)n\big)\theta\big] \\
& + B7_{\alpha(2+6\beta)}(\tau)\sin\big[\big(\alpha N-(\overline{N}_2-\alpha)n\big)\theta\big] + A8_{\alpha(2+6\beta)}(\tau)\cos\big[\big(\alpha N+(\overline{N}_2-\alpha)n\big)\theta\big] \\
& + B8_{\alpha(2+6\beta)}(\tau)\sin\big[\big(\alpha N+(\overline{N}_2-\alpha)n\big)\theta\big]\Big\}\times \\
& \left\{-\frac{(3+6\beta)}{(4+12\beta)}\cos(6\beta m\pi\varepsilon) + \cos[(2+6\beta)m\pi\varepsilon] - \frac{(1+6\beta)}{(4+12\beta)}\cos[(4+6\beta)m\pi\varepsilon]\right\}
\end{aligned}
\tag{7}
$$

The additional terms in Eq. (7) are due to the quadratic and cubic nonlinearities in the equations of motion. By retaining in Eq. (7) a sufficient number of terms to achieve convergence up to large vibration amplitudes [12], substituting this approximate expansion into Eq. (2) and solving analytically the partial differential equation, a consistent solution for the stress function F is obtained. Finally, by substituting the adopted expansion for the transversal displacement together with the obtained stress function into the Eq. (1) and by applying the standard Galerkin method, a discretized system of ordinary differential equations of motion is derived.

3   NUMERICAL RESULTS

The results presented here are for a cylindrical shell made of homogeneous and isotropic material with E = 210 GPa, ν = 0.3 and ρ = 7850 kg/m³ with dimensions R = 0.2 m, L = 0.34163 m and h = 0.002 m. The linear viscous damping coefficient, β_1, is 0.001 and the viscoelastic material damping, β_2, is 0.0001. It is known from section 2.2 that, for this geometry, the cylindrical shell may display a modal interaction between modes $(m, n) = (1, 5)$ and $(m, N) = (1, 6)$.

In order to understand the influence of the modal interaction on the nonlinear behavior of the shell, the three following modal expansions are obtained from Eq. (7):

1.   Model 1 - $(m, n) = (1, 5)$

9 D.O.F $- A1_{11}(\tau) + B1_{11}(\tau) + A5_{02}(\tau) + A5_{22}(\tau) + B5_{22}(\tau) + A1_{13}(\tau) + B1_{13}(\tau) + A1_{31}(\tau) + B1_{31}(\tau)$.

2.   Model 2 - $(m, N) = (1, 6)$

9 D.O.F $- A2_{11}(\tau) + B2_{11}(\tau) + A6_{02}(\tau) + A6_{22}(\tau) + B6_{22}(\tau) + A2_{13}(\tau) + B2_{13}(\tau) + A2_{31}(\tau) + B2_{31}(\tau)$.

3.   Model 3 - $(m, n) + (m, N) = (1, 5) + (1, 6)$

29 D.O.F $- A1_{11}(\tau) + B1_{11}(\tau) + A2_{11}(\tau) + B2_{11}(\tau) + A5_{02}(\tau) + A5_{22}(\tau) + B5_{22}(\tau) + A6_{22}(\tau) + B6_{22}(\tau) + \mathbf{A7_{12}(\tau)} + \mathbf{B7_{12}(\tau)} + \mathbf{A8_{12}(\tau)} + \mathbf{B8_{12}(\tau)} + A1_{13}(\tau) + B1_{13}(\tau) + A2_{13}(\tau) + B2_{13}(\tau) + A1_{31}(\tau) + B1_{31}(\tau) + A2_{31}(\tau) + \mathbf{B2_{31}(\tau)} + \mathbf{A3_{11}(\tau)} + \mathbf{B3_{11}(\tau)} + \mathbf{A4_{11}(\tau)} + \mathbf{B4_{11}(\tau)} + \mathbf{A3_{21}(\tau)} + \mathbf{B3_{21}(\tau)} + \mathbf{A4_{21}(\tau)} + \mathbf{B4_{21}(\tau)}$.

Model 1 considers the two vibrations modes with $(m, n) = (1, 5)$ and the associated modes due to modal coupling. Model 2 is the modal expansion for the two modes with $(m, N) = (1, 6)$. Model 3 consists of the addition of models 1 and 2 plus the new modes due to their modal interaction, which are written in bold type.

In this work an axially pre-loaded cylindrical shell is analyzed. The initial pre-load of the shell is located between the critical static load, Γ_{0CR}, and the minimum post-critical load Γ_{min}, so that a three potential well function is obtained, and, the adopted value of the pre-load is Γ_0 = 0.50. For this load level the shells displays five static solutions: a fundamental, two stable and two unstable post-critical solutions [5, 13]. Both the principal and secondary instability regions − which are the most important regions in non-linear dynamic analysis − for modes $(m, n) = (1, 5)$ and $(m, n) = (1, 6)$, are located in the region $\Omega_f < 2$ due to the static pre-load [13]. Figure 2 displays both the parametric instability (PI) and permanent escape (PE) boundaries for different vibration modes (m, n). As can be observed, other vibration modes also influence the dynamics of the shell in this forcing region. In this figure, only the modes that influence the instability boundaries are displayed [13].

In Figure 2 the uncoupled modes $(m, n) = (1, 5)$ and $(m, n) = (1, 6)$ interact with modes $(m, n) = (1, 4)$ and $(m, n) = (2, 6)$ which influence strongly both the parametric instability and permanent escape boundaries. So, the interaction between modes $(m, n) = (1, 4)$ and $(m, n) = (2, 6)$ with modes $(m, n) = (1, 5)$ and $(m, n) = (1, 6)$ is considered in Model 1. The region located below the parametric instability boundary represents combinations of harmonic load amplitude, Γ_1, and load excitation frequency, Ω_f, that lead to trivial solutions. The region located between the parametric instability boundary and permanent escape boundary, displays nontrivial solutions within the pre-buckling safe well. This region is limited by the saddle points associated with the unstable post-critical solutions for the defined load level. The region above the permanent escape boundary, represents combinations of de Γ_1 e Ω_f that generate large amplitude cross-well vibrations or small vibrations within a post-buckling well.
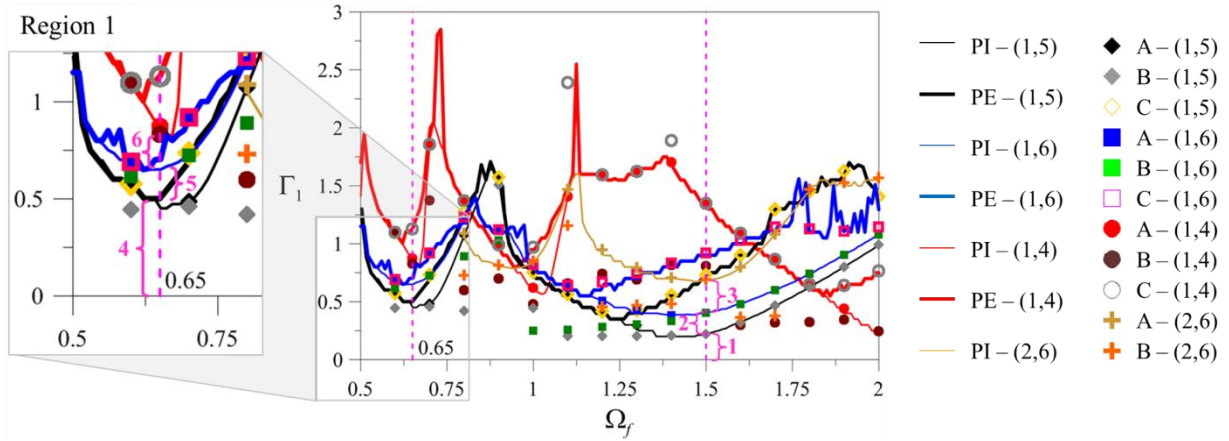
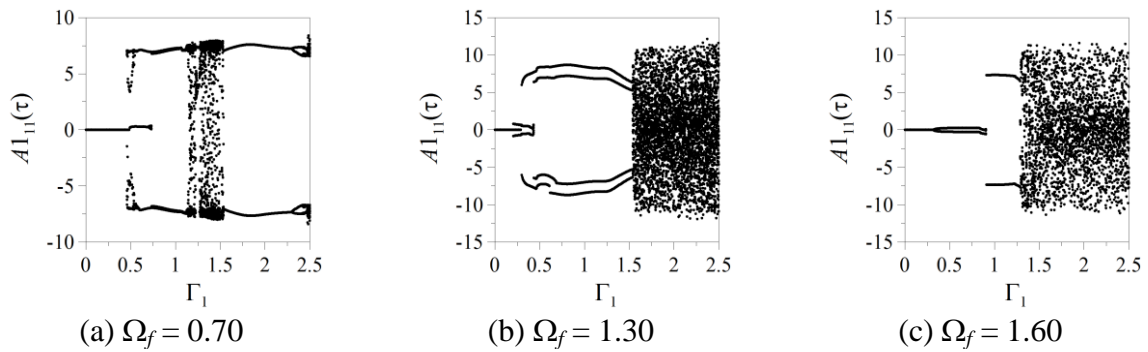Figure 2: Parametric instability and permanent escape boundaries for different uncoupled modes.

(a) $\Omega_f = 0.70$ (b) $\Omega_f = 1.30$ (c) $\Omega_f = 1.60$

Figure 3: Bifurcation diagrams for $(m, n) = (1, 5)$. $\Gamma_0 = 0.50$. Model 1.

(a) $\Omega_f = 0.70$ (b) $\Omega_f = 1.30$ (c) $\Omega_f = 1.60$
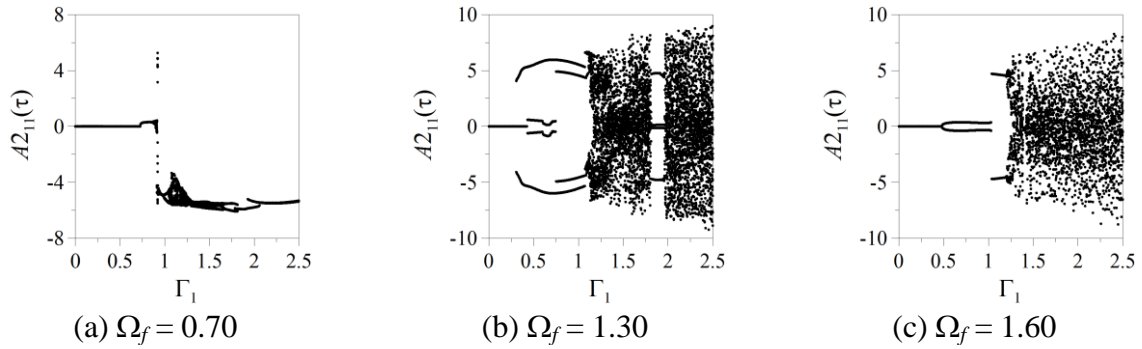
Figure 4: Bifurcation diagrams for $(m, n) = (1, 6)$. $\Gamma_0 = 0.50$. Model 2.

(a) $\Omega_f = 0.70$ (b) $\Omega_f = 1.30$ (c) $\Omega_f = 1.60$
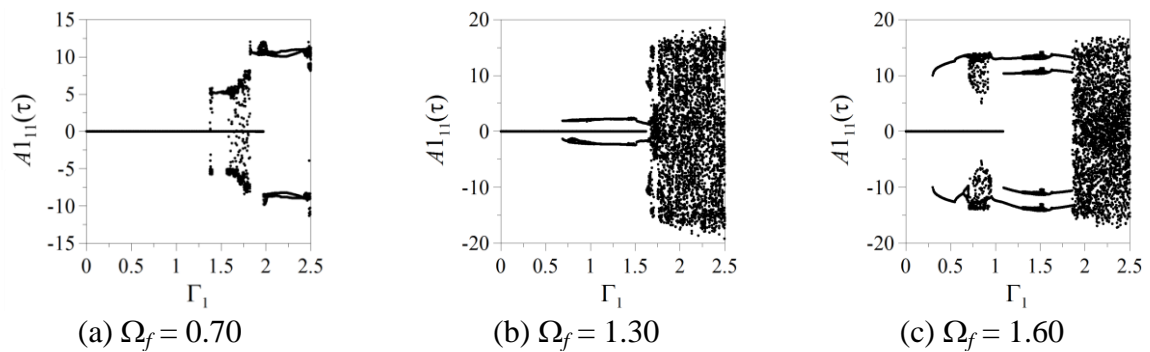
Figure 5: Bifurcation diagrams for $(m, n) = (1, 4)$. $\Gamma_0 = 0.50$. Model 1.

6

Figures 3 and 4 display the evolution of bifurcation diagrams for increasing forcing magnitude in the principal instability region using Models 1 and 2, both with 9 d.o.f. Figures 5 and 6 display the evolution of the bifurcation diagrams for vibration modes $(m, n) = (1, 4)$ and $(m, n) = (2, 6)$.
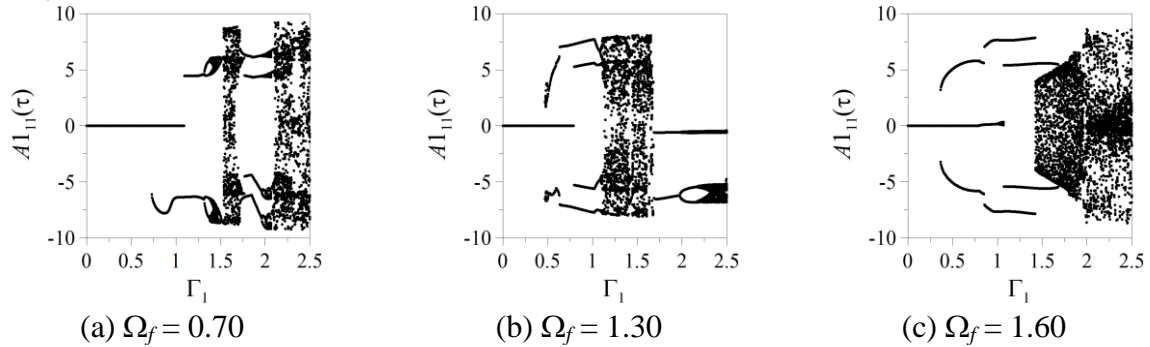

(a) $\Omega_f = 0.70$ (b) $\Omega_f = 1.30$ (c) $\Omega_f = 1.60$

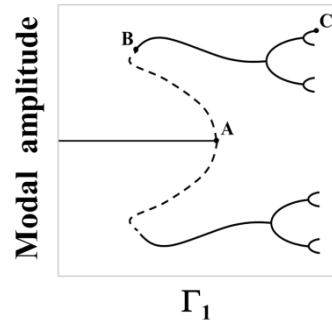Figure 6: Bifurcation diagrams for $(m, n) = (2, 6)$. $\Gamma_0 = 0.50$. Model 1.

Figure 7: Bifurcations of equilibrium solutions. — stable solutions and --- unstable solutions.

From Figures 3 to 6 it is possible to observe that the bifurcation diagrams display a complex evolution of stable solutions. For example, if the bifurcation diagrams of four different models are considered with $\Omega_f = 1.60$, Figures 3-6(c), it can be observed that, for the same load level and forcing frequency (Ω_f, Γ_1), trivial, periodic, quasi-periodic and even chaotic solutions coexist. So, it is important to study the influence of each mode on the bifurcation scenario.

In all cases the trivial solution becomes unstable due to a subcritical period doubling bifurcation. A typical bifurcation diagram is shown in Fig. 7 where the bifurcation points **A**, **B** and **C** are identified. Point **A** represents the parametric instability point. Point **B** represents the point where the first saddle-node bifurcation appears. Finally, Point **C** represents escape from the pre-buckling well [13]. Points **A**, **B** and **C** for each uncoupled modes are displayed in Figure 2. So, even before the parametric instability boundary is attained, nontrivial solutions may occur due to the sub-critical period-doubling bifurcations of each uncoupled mode.

(a) basic of attraction
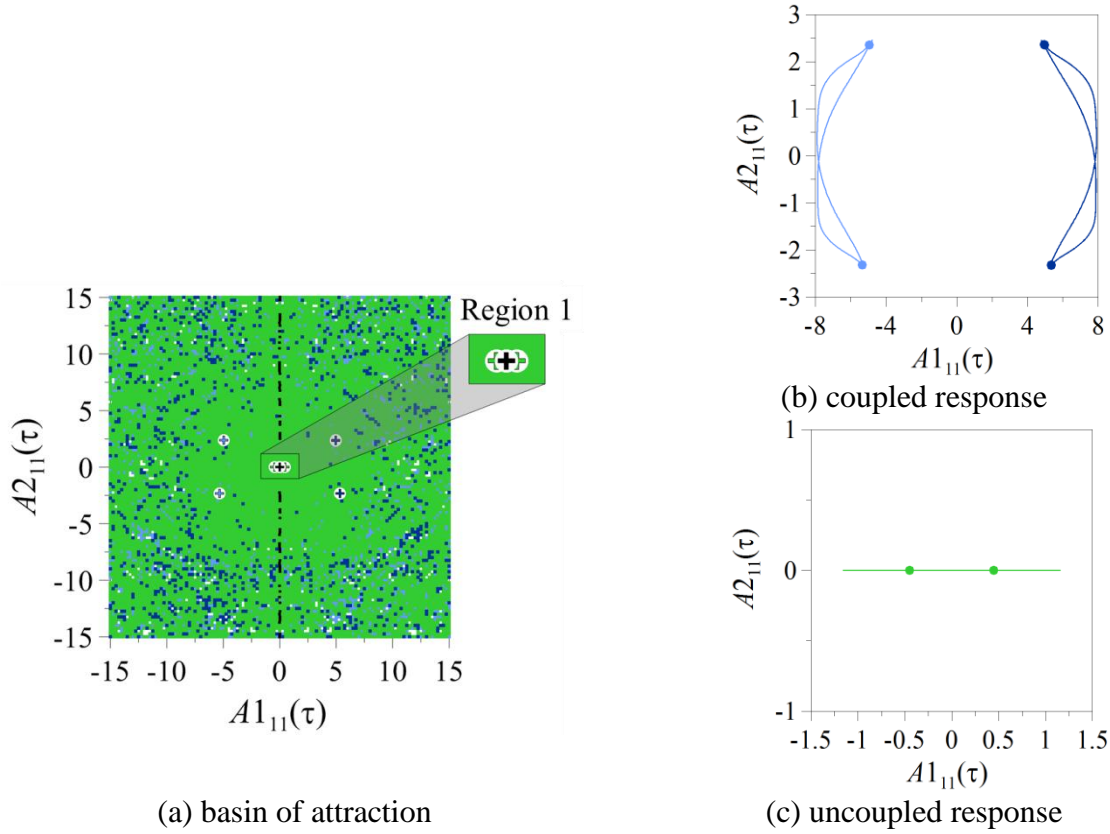
(b) coupled response

(c) uncoupled response

Figure 8: Basin of attraction and phase portrait. Model 3. $\Gamma_0 = 0.50$, $\Omega_0 = 1.50$ and $\Gamma_1 = 0.30$.

Figures 8a and 9a display a cross section of the basin of attraction by the plane $A1_{11}(\tau)$ x $A2_{11}(\tau)$ considering $\Gamma_0 = 0.50$, $\Omega_0 = 1.50$ and $\Gamma_1 = 0.30$ (Figure 8a) and $\Gamma_1 = 0.50$ (Figure 9a). These basins of attraction were obtained considering Model 3 (coupled model). Observing the dashed vertical line at $\Omega_0 = 1.50$, it is observed that, before the saddle-node bifurcation of mode $(m, n) = (1, 5)$ only the trivial solution exists, after the saddle-node bifurcations at least two solutions coexist, the 2T solution of mode $(1, 5)$ and the trivial solution. After the saddle-node bifurcation of mode $(1, 6)$, at least three solutions coexists, the trivial one, the 2T solution of mode $(1, 5)$ and the 2T solution of mode $(1, 6)$, which are uncoupled solutions. The cross sections of basins of attraction by the planes $A1_{11}(\tau)$ x $A2_{11}(\tau)$ allows one to observe new stable coupled solutions which are not possible to identify in the bifurcation diagrams of uncoupled modes (Figures 3-6). From the phase portraits of Figures 8b and 9b, it is possible to observe that there are orbits coupling the displacements of classic modes $(1, 5)$ and $(1, 6)$, which coexists with the uncoupled nontrivial solutions (Figures 8c and 9c). A similar behavior can be observed for $\Omega_0 = 0.65$ in Figure 2 (secondary region of instability) where new solutions arise due to modal interaction between modes $(1, 5)$ and $(1, 6)$.

8

(a) basin of attraction

(b) coupled response

(c)uncoupled responses
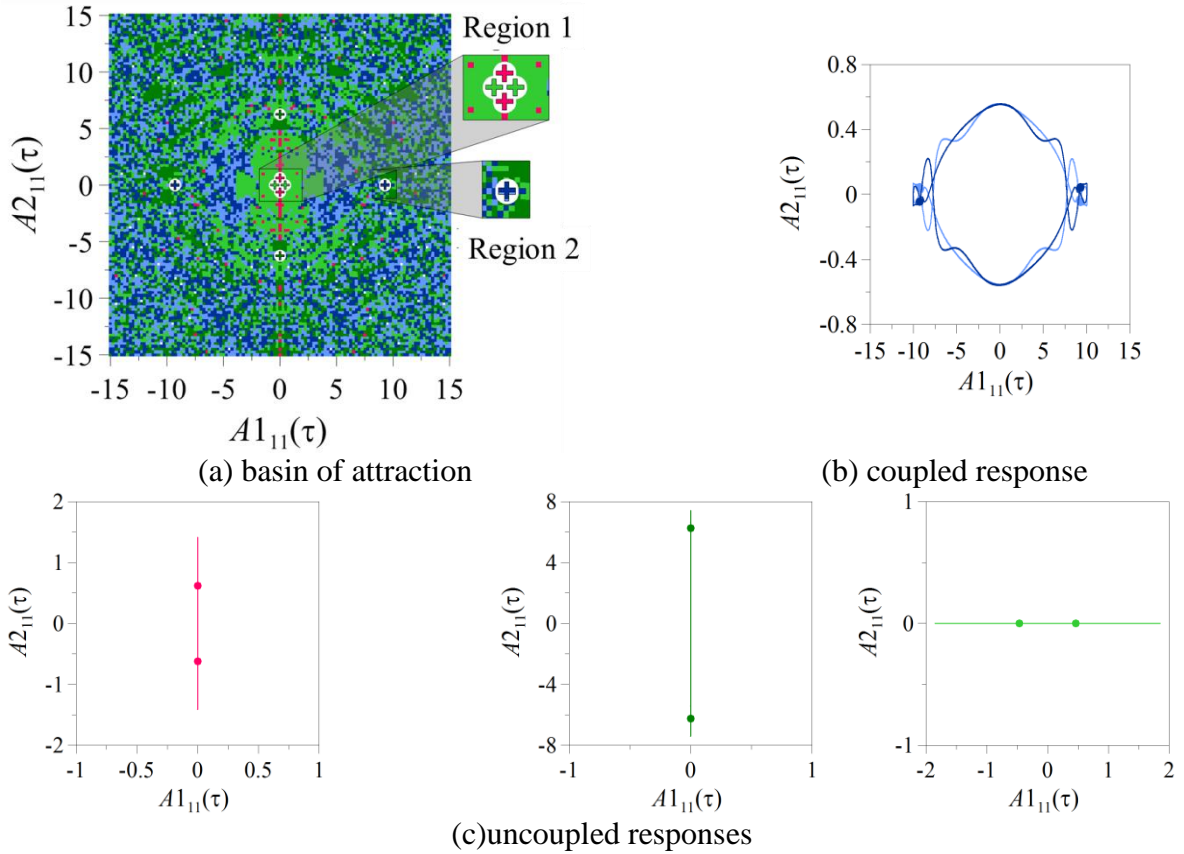
Figure 9: Basin of attraction and phase portraits. Model 3. $\Gamma_0 = 0.50$, $\Omega_0 = 1.50$ and $\Gamma_1 = 0.50$.

4 CONCLUSIONS

In the present paper, the influence of the nonlinear interaction among four neighbor modes with the same natural frequency, leading to a 1:1:1:1 internal resonance, on the stability of a cylindrical shell under axial load is studied. To model the shell, the Donnell nonlinear shallow shell theory is used. Based on a perturbation procedure, a general solution for the transversal displacement field considering the interaction among these modes is obtained which satisfies the boundary conditions of a simply-supported shell. Precise low dimensional models considering or not the modal interaction are derived and results are compared. The results show that the modal interaction among these modes with the same or nearly the same natural frequencies, a phenomenon observed in many practical shell geometries, may lead to many unsafe nonlinear phenomena, such as unstable bifurcations and jumps. Consequently, this must be considered for a safe shell design in a dynamic environment. Of course, due to the complexity of the nonlinear shell vibration observed in the present work and the dense frequency spectrum of shell structures, additional research must be conducted to unveil the influence of modal interaction in the nonlinear shell dynamics. Highly fractal basins of attraction are obtained leading to a high sensitivity to initial conditions and disturbances which may lead to several jumps between competing solutions, with sudden variations in the shell stress field.

REFERENCES

[1] G.W. Hunt, K. A. J Williams, R. G. Cowell, Hidden symmetry concepts in the elastic buckling of axially loaded cylinders, *International Journal of Solid and Structures*, **22**, 1501-1515, 1986.

[2] H. N. Chu, Influence of large amplitudes on flexural vibrations of a thin circular cylindrical shells, *Journal of Aerospace Science*, **28**, 302-609, 1961.

[3] J. L. Nowinski, Nonlinear transverse vibration of orthotropic cylindrical shells, *AIAA Journal*, **1**, 617-620, 1963.

[4] D. A. Evensen, Some observations on the nonlinear vibration of thin cylindrical shells, *AIAA Journal*, **1**, 2857-2858, 1963.

[5] N. Yamaki, *Elastic stability of cicurlar cylindrical shells*, North-Holland Series in Applied Mathematics and Mechanics, 558p, 1984.

[6] M. Amabili, M. P. Païdoussis, Review of studies on geometrically nonlinear vibrations and dynamics of circular cylindrical shells and panels, with and without fluid-structure interaction, *Applied Mechanics Reviews*, **56**, 655-699, 2003.

[7] P. B. Gonçalves, R. C. Batista, Nonlinear vibration analysis of fluid-filled cylindrical shells, *Journal of Sound and Vibration*, **127**, 133-143, 1988.

[8] A. A. Popov, J. M. T. Thompson, F. A. McRobie, Low dimensional models of shell vibrations: parametrically excited vibrations of cylindrical shells, *Journal of Sound and Vibration*, **209**, 163-186, 1998.

[9] Z. J. G. N. Del Prado, *Modal coupling and interaction in the dynamic instability of cylindrical shells* (in Portuguese). Ph. D. Thesis, Civil Engineering Department, Catholic University, PUC-Rio, Rio de Janeiro, Brazil, 2001.

[10] P.B. Gonçalves, Z. J. G N. Del Prado, Effect of non-linear modal interaction on the dynamic instability of axially excited cylindrical shells, *Computers and Structures*, **82**, 2621-2634, 2004.

[11] M. Amabili, Internal resonances in non-linear vibrations of laminated circular cylindrical shell, *Nonlinear Dynamics*, **69**, 755-770, 2012.

[12] P. B. Gonçalves, F. M. A Silva, Z. J. G. N. Del Prado, Low-dimensional models for the nonlinear vibration analysis of cylindrical shells based on a perturbation procedure and proper orthogonal decomposition, *Journal of Sound and Vibration*, **315**, 641-663, 2008.

[13] L. Rodrigues, *An introduction about the modal interaction on the nonlinear oscillations of cylindrical shells* (in Portuguese). Master thesis, School of Civil Engineering, Federal University of Goiás, 2013.